Visualizing localized reentry with ultra-high density mapping in iatrogenic atrial tachycardia – beware pseudo-reentry.

Running title: Localized reentry in ultra-high density

Vishal Luther MRCP[1]*; Markus Sikkel MRCP PhD[1]*; Nathan Bennett MEng[2]; Fernando Guerrero BSc[2]; Kevin Leong MRCP[1], Norman Qureshi MRCP[1]; Fu Siong Ng MRCP, PhD[1]; Sajad A Hayat, MRCP PhD[1]; Afzal Sohaib MRCP PhD[1]; Louisa Malcolme-Lawes MRCP PhD[1]; Elaine Lim BSc[1]; Ian Wright BSc[1]; Michael Koa-Wing MRCP PhD[1], David C. Lefroy MA FRCP; Nick WF Linton MEng, MRCP, PhD[1]; Zachary Whinnett MRCP, PhD[1]; Prapa Kanagaratnam FRCP, PhD[1]; D. Wyn Davies MD, FRCP, FHRS[1]; Nicholas S. Peters MD, FRCP, FHRS[1]; Phang Boon Lim MRCP, PhD[1]

* Joint first authors

Institutional Affiliation:

1. Imperial College Healthcare NHS Trust, Hammersmith Hospital, Department of Cardiology, Du Cane Road, London W12 0HS, United Kingdom.

2. Boston Scientific Ltd, 300 Boston Scientific Way, Marlborough, Massachusetts, 01752-1234

Corresponding Author: Dr Phang Boon Lim.

Cardiology Dept, 2nd Floor, B Block, Hammersmith Hospital, Du Cane Road, London, United Kingdom, W12 0HS.

Telephone: +44 (0) 203 313 4967 Fax: +44 (0) 203 313 4095 Email: pblim@imperial.ac.uk

Journal Subject Terms

Arrhythmia and Electrophysiology

- Arrhythmias

- Catheter Ablation and Implantable Cardioverter-Defibrillator
- Atrial Fibrillation
- Electrophysiology

Word count: 6127

Abstract

Background: The activation pattern of localized re-entry (LR) in atrial tachycardia (AT) remains incompletely understood. We used the ultra-high density Rhythmia™ mapping system to study activation patterns in LR.

Methods and Results: LR was suggested by small rotatory activations (carousels) containing the full spectrum of the color-coded map. 23 left sided ATs were mapped in 15 patients (age 64±11yrs). 16,253 ± 9,192 points were displayed per map, collected over 26±14mins. A total of 50 carousels were identified (median 2, quartiles 1-3 per map), though this represented LR in only n=7/50 (14%): here, rotation occurred around a small area of scar (<0.03mV, 12±6mm diameter). In LR, electrograms along the carousel encompassed the full TCL and surrounding activation moved away from the carousel in all directions. Ablating fractionated electrograms (117±18ms; 44±13% of TCL) within the carousel interrupted the tachycardia in every LR case. All remaining carousels were pseudo-reentrant (n=43/50 (86%)) occurring in areas of wavefront collision (n=21, median 0.5, quartiles 0-2 per map); or as artifact due to annotation of noise or interpolation in areas of incomplete mapping (n=22; median 1, quartiles 0-2 per map). Pseudo-reentrant carousels were incorrectly ablated in 5 cases having been misinterpreted as LR.

Conclusion: The activation pattern of LR is of small stable rotational activations (carousels), and this drove 30% (7/23) of our post ablation ATs. However, this appearance is most often pseudo-re-entrant, and must be differentiated by interpretation of electrograms in the candidate circuit and activation in the wider surrounding region.

Key words: Atrial tachycardia, re-entry, scar, high-density mapping, Rhythmia

Introduction

The classification of an Atrial Tachycardia (AT) is defined by its intra-cardiac activation pattern as seen whilst mapping. A "focal" AT demonstrates centrifugal activation away from a discrete region, and a "macro-reentrant" AT demonstrates progressive activation around the cardiac chamber covering the full tachycardia cycle length (TCL).[1] A more recently classified AT is localized reentry (LR), seen most often post previous ablation, presumed to involve slow conduction and reentry around a small area of scar (less than 2cm in diameter).[2, 3] LR has been characterized by long duration and fractionated electrograms within the circuit spanning approximately 50% of the TCL. However, owing to the limited number of points acquired with most mapping systems, as well as the difficulty annotating activation times in areas of slow conduction, the activation pattern of LR is usually inferred rather than accurately delineated.[4-6]

Recently, a multi-electrode basket catheter has been developed which comprises 64 mini-electrodes (Orion™, Boston Scientific, Cambridge, MA) paired to a 3D mapping system (Rhythmia™, Boston Scientific).[7] The system offers "ultra-high" electro-anatomical point density (often in excess of 10,000 points per map) and improved electrogram resolution for activation mapping.[8] This has enabled a better understanding of different tachycardia circuitry, especially within low voltage myocardium.[9, 10] In this study, we hypothesized that the system could accurately delineate the activation of localized reentry in iatrogenic ATs as a guide to ablation.

Methods

Patients with symptomatic ATs post previous AF ablation referred to our center and mapped with Rhythmia™ were studied. The catheter and mapping system has been previously described in detail.[7] The study was approved by an institutional review committee and all subjects gave informed consent.

Procedures were conducted under general anesthesia. A decapolar catheter was placed in the coronary sinus and used as a stable reference to time local activation in tachycardia. Transseptal access was gained to the left atrium using trans-esophageal echocardiography, and the Orion™ catheter and ablation catheter were supported using long sheaths. Unfractionated heparin was administered prior to insertion of the Orion™ catheter through an 8.5F sheath and continued to maintain an activated clotting time greater than 300sec throughout.

The geometry of the cardiac chambers was acquired based on the location of the outer-most electrodes of the basket using in-built magnetic and impedance sensing. Mapping was performed in tachycardia, seen either from the start, or induced with atrial burst pacing. The system calculated the median TCL over 10sec and set the duration of the window of interest (WOI) to 100% of the observed cycle length, centered on the timing reference electrode. Beats were automatically and continuously collected, and were only accepted for display on the map having passed through a series of beat acceptance criteria: a stable cycle length within 10ms of the target TCL; relative timing deviation of 5ms between 2 coronary sinus reference electrodes; respiration gating in expiration phase with a threshold set at 50% of the peak-peak amplitude; stable catheter location within 1mm; and stability of the mapping catheter signal morphology of at least 75% from beat to beat. Only electrograms within 2mm of the surface geometry were displayed and used for map computation.

The system displayed activation around the cardiac chamber by measuring the "local activation time" (LAT) at different sites in relation to a stable reference, presenting this information on a color coded map. The annotation of local activation time was assigned automatically by the system, based on either the bipolar or unipolar electrogram signal. For bipolar maps, electrograms with a single component were annotated at the maximum absolute peak of the bipolar electrogram. For electrograms with more than 1 potential, annotation was guided by surrounding electrograms. For unipolar maps, activation was annotated at the maximal negative unipolar derivative corresponding with a relevant bipolar activation. Individual electrograms and their annotation of activation timing could be studied by roving a virtual probe incorporated within system at the desired location. No manual re-annotation of activation time was performed.

The WOI was represented as a color wheel running from red to purple, and spanning the colors of the rainbow. These limits defaulted to red being the earliest in the window and purple being the latest. However by representing the color bar as a wheel, purple conveyed activation 10ms before red for reentrant maps. These limits could be rotated around the color wheel, and this had the equivalent effect of sliding the WOI without causing a full map re-compute. This function preserved the full color spectrum on the propagation map. Wavefront activation could be followed by rotating the color wheel and tracking the leading edge of a maroon colored wavefront, distinguishable from the rainbow spectrum, around the cardiac chamber. Activation in regions of extremely low voltage and/or inconsistent timing between neighboring points could be hidden from the map using a "confidence mask". The default threshold of 0.03mV was used in this study, and areas below this confidence threshold were displayed in gray and defined as scar. Reducing this value below <0.03mV reduced the gray zone size.

Theoretically, LR should demonstrate continuous rotation within a small area, with each rotation encompassing one full TCL. We identified all putative LR sites as those with apparent continuous rotational activation around an area <2cm (based on the mapping field of the multi-spline catheters in which LR was originally mapped).[2] We labeled these rotational patterns as "carousels." These sites spanned the full spectrum of the color coded map, with an early (red) meets late (purple) site. An example is illustrated in figure 1 and supplementary video 1. For each putative LR site, the electrograms along the rotation were studied. We defined localized reentry where:

1) Electrograms could be tracked around the circuit and spanned the complete tachycardia cycle length without any unaccounted-for isoelectric period.

2) Activation moved away from the circuit in all direction.

3) The appearance of rotation was consistent between unipolar and bipolar LAT maps.

4) Termination of tachycardia with ablation within the circuit

Entrainment maneuvers were generally avoided owing to the risk of transforming or terminating the tachycardia, and because local capture within low voltage areas may have proved difficult. A fractionated electrogram within the circuit was targeted for ablation. Power controlled (25–35W) radiofrequency (RF) energy was delivered (Stockert^{TM} 70 RF generator, Biosense Webster) through an irrigated ablation catheter (17mL/min) with a target temperature of 48 ◦C

Statistics: Categorical variables were expressed as percentages. Continuous variables were expressed as mean ± 1 standard deviation for data with symmetric distributions and/or medians with first and third quartiles for skewed distributions.

Results

A total of 23 left ATs were fully mapped in 15 patients (age 64±11yrs) using ultra-high density (16,253 ± 9,192 points displayed per map). Each patient had undergone previous atrial fibrillation (AF) ablation (pulmonary venous isolation (100%), roof line 8/15 (53%) mitral isthmus line 5/15 (33%), electrogram defragmentation 5/15 (33%)), and 11/15 (73%) patients had undergone 2 or more ablation procedures including 5/15 (33%) for a previous AT. The mean AT cycle length mapped was 279±76ms, 8 of which were induced (either initially or post termination of a different AT). The mean LA volume was 133±37cc, collected from 2197±1649 beats over an average mapping time of 26±14mins.

We identified n=50 carousels (median 2, quartiles 1-3 per map) in these 23 maps. Table 1 summarizes the clinical details, past procedure history and the number of carousels per patient. Three distinct carousel types were identified and a decision tree to classify carousel activation is presented in figure 1.

Type 1 Carousel – localized re-entry: This was observed in n=7/50 carousels (14%). Examples are presented in figures 2&3 and supplementary videos 2&3. Electrograms tracked around the circuit encompassed the full TCL. Of these 7 carousels, n=6 appeared to rotate around an area of probable scar, colored gray in the map, defined by a peak amplitude <0.03mV or inconsistent activation timing between neighbouring points. The size of the scar was found to be smaller than previous studies have suggested (max. diameter 12±6mm; median surface area 44mm^2 (quartiles =31-55)). The remaining n=1 rotated through two distinct gaps along a line of block (2cm in length). Conduction velocity around the scar varied in accordance with degree of fractionation along the carousel. The activation wavefront in the wider area around the carousel moved away

in all directions. Carousel activation was consistent at the same site on both unipolar and bipolar display (as illustrated in the supplementary figures corresponding to figures 2&3). The most fractionated electrogram along the carousel (117±18ms; 44±13% of TCL) was ablated resulting in termination of AT in every case, confirming that this activation was consistent with LR. Figure 2 illustrates how iatrogenic LR can occur following previous ablation.

Type II Carousel - pseudo-reentry: This was observed in n=21/50 (42%) carousels (median 0.5, quartiles 0-2 per map, identified in 8/23 AT maps). Examples are presented in figures 4&5 and supplementary videos 4&5. As the head of an activation wavefront entered a region of low voltage, it slowed and curved around this site. A secondary wavefront was seen to enter this region from elsewhere, colliding with the head of the primary wavefront and advancing activation around it. This complex wavefront interaction created a visual impression of rotation, which we classified as pseudo-reentrant. This carousel was characterized by overlapping regions of split or fractionated potentials coinciding with wavefront collision, highlighted by the color heterogeneity of the points annotated within this region (indicative of adjacent electrograms with different activation timings). Electrograms could not be tracked around the full TCL, owing to the unaccounted for isoelectric period between the split potentials. All electrogram signals were real, hence the carousel activation was consistent at the same site on both unipolar and bipolar activation maps (as illustrated in the supplementary figures corresponding to figures 4&5). These carousels were misdiagnosed as localized re-entrant in 5 cases, and inappropriately ablated (an example is illustrated in figure 5).

Type III carousel – artifact: This was observed in n=22/50 (44%) carousels (median 1, quartiles 0-2 per map, identified in 10/23 AT maps). A pinwheel was often present at the center of rotation. These occurred due to annotation of artifact signal in areas of incomplete mapping. Less detailed mapping was performed immediately adjacent to the mitral annulus and isolated pulmonary veins, where these carousels were typically found. As illustrated in figure 6 and supplementary video 6, just 3 points with different local activation times across the WOI can create the appearance of continuous rotation owing to interpolation of activation between these sites. Figure 7 and supplementary video 7 illustrates how annotation of noise was able to create carousel activation near the mitral annulus. Real electrograms could not be tracked around the full TCL. Carousel activation was inconsistent between unipolar and bipolar activation maps (as illustrated in the supplementary figures corresponding to figures 7). In many of these carousels, activation could be observed heading into them from elsewhere. These carousels were easily recognizable as an interpolation error and never ablated.

Further examples of each carousel type are presented as ***additional*** supplementary videos (1-3).

Discussion

This study used ultra-high density mapping with increased electrogram resolution to characterize the activation pattern of LR in AT. Activation appeared as a stable and continuous rotation around a small island of scar (approximately 1cm in diameter) that encompassed the full TCL. However, this pattern of activation had poor specificity, and more commonly occurred in areas of wavefront turning and collision or due to annotation of artifact. This study illustrates how both the electrograms in the candidate circuit as well as activation in the wider surrounding region are necessary to distinguish pseudo from localized reentry.

Extensive left atrial ablation in the treatment of persistent AF is associated with future AT.[11-13] Areas of recovery will conduct slowly, manifest by electrogram fractionation, and support the initiation and sustainability of LR.[14] Mapping local activation within regions of slow conduction has been limited by the resolution of electrogram signals recorded by conventional mapping catheters. Furthermore, limited point density on prior mapping systems resulted in large areas of activation interpolation, and localized re-entrant circuits often appeared as focal.[4, 5, 15, 16] Studies with multi-spline catheters suggested that LR involves reentry around an area of scar less than 2cm in diameter, corresponding to the mapping field of these specific catheters. The Rhythmia™ mapping system offers ultra-high density electro-anatomical mapping with increased electrogram resolution.[17] Combining 64 very small electrodes with narrow inter-electrode spacing (0.4 mm^2; 2.5 mm center-to-center spacing), as well as a point density >10 fold that of conventional maps, it facilitates the differentiation of active from non-conductive tissue within low voltage areas, critical to studying LR.[9, 10, 18] Using this system, we have been able to fully characterize the activation pattern of most LR circuits as small rotatory activations around scar approximately 1cm in diameter. We termed this type of activation a “carousel”.

Electrograms could be followed around the circuit and encompassed the full tachycardia cycle length. Ablation at sites of electrogram fractionation within the carousel interrupted the tachycardia in each case. With the expectant incorporation of ultra-high density facilities into most 3D mapping systems, this pattern of activation will be seen far more frequently.

However, carousels are not specific for LR. In this study, carousels were evident on most maps collected, though represented LR in only a small proportion. The majority of carousels were pseudo-reentrant. Where an activation wavefront curved around an area of non-uniform anisotropy, a critically timed secondary wavefront entering from the opposite direction collided and extinguished the primary wavefront, and advanced activation around it, creating the visual impression of rotational activation. Upon closer inspection, the exact nature of these wavefronts interactions was understood, akin to recurrent reset seen during entrainment, an observation facilitated by ultra-high density.[19, 20] These areas of collision contained overlapping regions of split or fractionated potentials. This appearance was distinct from LR where activation moved away in all directions. Without careful recognition of this phenomenon, operators may be misled to deliver ablation at these pseudo-reentrant sites irrelevant to the clinical tachycardia. Carousels also arose from annotation of artifact or interpolation in areas of incomplete mapping. In-fact, a minimum of three closely spaced points was sufficient to create this false carousel, where annotation happened to span the WOI. Such an occurrence might be seen in areas of electrogram fractionation (where the system must assign a single activation time to a multi-component signal), in areas with poor catheter contact, and in areas with a low signal to noise ratio.

The voltage threshold to differentiate atrial scar from conducting tissue is unknown. Studies using cardiac magnetic resonance imaging suggested regions below 0.3mV were consistent with chronically ablated atrial tissue.[21] Sites without pace capture (at 10mA/2ms) led

to a lower suggestion of 0.15mV.[22] The Rhythmia™ system includes a confidence mask which can be used to visually "gray out" areas of the map in which the system has a low confidence in its signal annotation either due to extremely low voltage, a locally large variation in annotation times or a mixture of both. Gray areas of the map may therefore suggest the presence of scar. Defining scar can be useful when mapping LR, and its accuracy is dependent on the recording technique and noise threshold of the mapping system. The greater fidelity mapping offered by the Rhythmia™ system allowed us to identify active tissue within areas of very low voltage, and apply a confidence mask threshold (or "scar threshold") of 0.03mV. This allowed us to identify regions of possible scar with amplitudes 5-10 times lower than previous studies about which LR can rotate. However, the confidence threshold is arbitrary, and 0.03mV was used as a default setting of the system. By reducing the threshold below 0.03mV, the central gray low confidence zone filled with color, and gave the false appearance of rotation anchored around a pinwheel. Despite the attraction of focusing ablation at the core of the pinwheel itself, operators should be cognizant that this appearance is an interpolation artifact, and that ablation at the exact pinwheel site is unlikely to terminate tachycardia.

This study has indirect implications for mapping of AF. Previous studies have suggested that AF may be driven by small rotational activations, manifest as early-to-late activating spirals with rotational activity around an anchor, akin to the carousels seen in this study.[23, 24] However, "localized re-entry" in AT and "rotors" in AF are mechanistically different and mapped using different techniques. Despite this difference, the visual impression of small rotational activations seen in both rhythms is similar, perhaps allowing for indirect comparison. The ablation of rotational activation in AF has had mixed clinical benefit.[25] We have shown that even in stable AT, the majority of rotational activation patterns seen are pseudo-reentrant, associated with

complex wavefront interactions. We incorrectly ablated these patterns, believing they represented LR. Wavefront collisions and interactions around lines of block are even more prevalent in a fibrillatory milieu, and this might lead to multiple "wannabe reentries" being incorrectly labeled as a rotor, and incorrectly ablated as well.[26]

Limitations

This is a single-center study with a limited number of patients. However, this study is not intended to be an experiential description of ultra-high density activation mapping, but rather offers a detailed analysis and pitfalls of identifying rotational activation in areas of low voltage.

We did not perform entrainment maneuvers within the localized re-entrant circuit owing to this risk of transforming or terminating the clinical tachycardia and because local capture within these low voltage areas may have proved difficult. A comparison of the response to entrainment within the carousel types would have offered greater understanding of their electrophysiological characteristics. However, our primary aim was to accurately delineate the 3D activation pattern of localized reentry with ultra-high density.

We used the conventional bipolar voltage metric to define scar, though changes in amplitude of a bipolar signal can occur according to the electrode orientation, wavefront direction, wavefront collision and atrial rate. Furthermore, there is no practical lower bound on voltage that defines a lack of conduction.

The most fractionated electrograms in these localized circuits were less than 50% of the full cycle length. A circuit with even longer duration of fractionation might occupy so much of the timing window at a single point that the full color spectrum may not be apparent. These micro-reentrant circuits may appear focal with very slow breakout away from its source. [3, 5]

Conclusions

Ultra-high density mapping is unique in its ability to display the activation of localized re-entrant AT in the previously-ablated left atrium. Activation is akin to a carousel, rotating around areas of scar (approximately 1cm in diameter), encompassing the full tachycardia cycle length with each rotation. However, carousel activation does not always imply LR, and occurs more commonly in areas of wavefront turning and collision or due to annotation of artifact. In the era of ultra-high density mapping of complex arrhythmia, rotational activation patterns should be interpreted with caution.

Funding sources

V. Luther is funded by a British Heart Foundation Clinical Research Training Fellowship award (no. FS/15/12/31239). M.B. Sikkel is supported by a National Institute of Health Research Clinical Lectureship award (#2670). We acknowledge the ElectroCardioMaths Programme of the British Heart Foundation Centre of Research Excellence, BHF Grant RG/10/11/28457, and the National Institute for Health Research (UK) Biomedical Research Centre.

Disclosures:

P.B.Lim has received speakers fee and research grant support from Boston Scientific.

References

1. Saoudi N, Cosio F, Waldo A, Chen SA, Iesaka Y, Lesh M, Saksena S, Salerno J, Schoels W. A classification of atrial flutter and regular atrial tachycardia according to electrophysiological mechanisms and anatomical bases; a statement from a joint expert group from the working group of arrhythmias of the european society of cardiology and the north american society of pacing and electrophysiology. *Eur Heart J*. 2001;22:1162-1182
2. Sanders P, Hocini M, Jais P, Hsu LF, Takahashi Y, Rotter M, Scavee C, Pasquie JL, Sacher F, Rostock T, Nalliah CJ, Clementy J, Haissaguerre M. Characterization of focal atrial tachycardia using high-density mapping. *J Am Coll Cardiol.* 2005;46:2088-2099
3. Jais P, Matsuo S, Knecht S, Weerasooriya R, Hocini M, Sacher F, Wright M, Nault I, Lellouche N, Klein G, Clementy J, Haissaguerre M. A deductive mapping strategy for atrial tachycardia following atrial fibrillation ablation: Importance of localized reentry. *J Cardiovasc Electrophysiol*. 2009;20:480-491
4. Ju W, Yang B, Chen H, Zhang F, Zhai L, Cao K, Chen M. Localized reentry as a novel type of the proarrhythmic effects of linear ablation in the left atrium. *Pacing Clin Electrophysiol*. 2011;34:919-926
5. Takahashi Y, Takahashi A, Miyazaki S, Kuwahara T, Takei A, Fujino T, Fujii A, Kusa S, Yagishita A, Nozato T, Hikita H, Sato A, Hirao K, Isobe M. Electrophysiological characteristics of localized reentrant atrial tachycardia occurring after catheter ablation of long-lasting persistent atrial fibrillation. *J Cardiovasc Electrophysiol*. 2009;20:623-629
6. Ikeguchi S, Peters NS. Novel use of postpacing interval mapping to guide radiofrequency ablation of focal atrial tachycardia with long intra-atrial conduction time. *Heart Rhythm*. 2004;1:88-93
7. Nakagawa H, Ikeda A, Sharma T, Lazzara R, Jackman WM. Rapid high resolution electroanatomical mapping: Evaluation of a new system in a canine atrial linear lesion model. *Circ Arrhythm Electrophysiol*. 2012;5:417-424
8. Schaeffer B, Hoffmann BA, Meyer C, Akbulak RO, Moser J, Jularic M, Eickholt C, Nuhrich JM, Kuklik P, Willems S. Characterization, mapping and ablation of complex atrial tachycardia: Initial experience with a novel method of ultra high-density 3d mapping. *J Cardiovasc Electrophysiol*. 2016;27:1139-1150
9. Anter E, McElderry TH, Contreras-Valdes FM, Li J, Tung P, Leshem E, Haffajee CI, Nakagawa H, Josephson ME. Evaluation of a novel high-resolution mapping technology for ablation of recurrent scar-related atrial tachycardias. *Heart Rhythm*. 2016;13:2048-2055
10. Anter E, Tschabrunn CM, Buxton AE, Josephson ME. High-resolution mapping of post-infarction reentrant ventricular tachycardia: Electrophysiological characterization of the circuit. *Circulation*. 2016;134:314-327
11. Chae S, Oral H, Good E, Dey S, Wimmer A, Crawford T, Wells D, Sarrazin JF, Chalfoun N, Kuhne M, Fortino J, Huether E, Lemerand T, Pelosi F, Bogun F, Morady F, Chugh A. Atrial tachycardia after circumferential pulmonary vein ablation of atrial fibrillation: Mechanistic insights, results of catheter ablation, and risk factors for recurrence. *J Am Coll Cardiol*. 2007;50:1781-1787
12. Haissaguerre M, Hocini M, Sanders P, Sacher F, Rotter M, Takahashi Y, Rostock T, Hsu LF, Bordachar P, Reuter S, Roudaut R, Clementy J, Jais P. Catheter ablation of long-lasting persistent atrial fibrillation: Clinical outcome and mechanisms of subsequent arrhythmias. *J Cardiovasc Electrophysiol*. 2005;16:1138-1147
13. Luther V, Linton NW, Koa-Wing M, Lim PB, Jamil-Copley S, Qureshi N, Ng FS, Hayat S, Whinnett Z, Davies DW, Peters NS, Kanagaratnam P. A prospective study of ripple mapping in atrial

tachycardias: A novel approach to interpreting activation in low-voltage areas. *Circ Arrhythm Electrophysiol*. 2016;9:e003582
14. Yokokawa M, Latchamsetty R, Ghanbari H, Belardi D, Makkar A, Roberts B, Saint-Phard W, Sinno M, Carrigan T, Kennedy R, Suwanagool A, Good E, Crawford T, Jongnarangsin K, Pelosi F, Jr., Bogun F, Oral H, Morady F, Chugh A. Characteristics of atrial tachycardia due to small vs large reentrant circuits after ablation of persistent atrial fibrillation. *Heart Rhythm*. 2013;10:469-476
15. Shah D, Sunthorn H, Burri H, Gentil-Baron P, Pruvot E, Schlaepfer J, Fromer M. Narrow, slow-conducting isthmus dependent left atrial reentry developing after ablation for atrial fibrillation: Ecg characterization and elimination by focal rf ablation. *J Cardiovasc Electrophysiol*. 2006;17:508-515
16. El Haddad M, Houben R, Tavernier R, Duytschaever M. Stable reentrant circuit with spiral wave activation driving atrial tachycardia. *Heart Rhythm*. 2014;11:716-718
17. Tschabrunn CM, Roujol S, Dorman NC, Nezafat R, Josephson ME, Anter E. High-resolution mapping of ventricular scar: Comparison between single and multielectrode catheters. *Circ Arrhythm Electrophysiol*. 2016;9: e003841
18. Hooks DA, Sacher F, Haissaguerre M, Derval N. Localized reentry within a previous mitral isthmus line ablation. *J Cardiovasc Electrophysiol*. 2016;27:232-233
19. Hanna MS, Coromilas J, Josephson ME, Wit AL, Peters NS. Mechanisms of resetting reentrant circuits in canine ventricular tachycardia. *Circulation*. 2001;103:1148-1156
20. Peters NS, Coromilas J, Hanna MS, Josephson ME, Costeas C, Wit AL. Characteristics of the temporal and spatial excitable gap in anisotropic reentrant circuits causing sustained ventricular tachycardia. *Circ res*. 1998;82:279-293
21. Harrison JL, Jensen HK, Peel SA, Chiribiri A, Grondal AK, Bloch LO, Pedersen SF, Bentzon JF, Kolbitsch C, Karim R, Williams SE, Linton NW, Rhode KS, Gill J, Cooklin M, Rinaldi CA, Wright M, Kim WY, Schaeffter T, Razavi RS, O'Neill MD. Cardiac magnetic resonance and electroanatomical mapping of acute and chronic atrial ablation injury: A histological validation study. *Eur Heart J*. 2014;35:1486-1495
22. Squara F, Frankel DS, Schaller R, Kapa S, Chik WW, Callans DJ, Marchlinski FE, Dixit S. Voltage mapping for delineating inexcitable dense scar in patients undergoing atrial fibrillation ablation: A new end point for enhancing pulmonary vein isolation. *Heart Rhythm*. 2014;11:1904-1911
23. Narayan SM, Krummen DE, Rappel WJ. Clinical mapping approach to diagnose electrical rotors and focal impulse sources for human atrial fibrillation. *J Cardiovasc Electrophysiol*. 2012;23:447-454
24. Haissaguerre M, Hocini M, Denis A, Shah AJ, Komatsu Y, Yamashita S, Daly M, Amraoui S, Zellerhoff S, Picat MQ, Quotb A, Jesel L, Lim H, Ploux S, Bordachar P, Attuel G, Meillet V, Ritter P, Derval N, Sacher F, Bernus O, Cochet H, Jais P, Dubois R. Driver domains in persistent atrial fibrillation. *Circulation*. 2014;130:530-538
25. Benharash P, Buch E, Frank P, Share M, Tung R, Shivkumar K, Mandapati R. Quantitative analysis of localized sources identified by focal impulse and rotor modulation mapping in atrial fibrillation. *Circ Arrhythm Electrophysiol*.2015;8:554-561
26. Lee S, Sahadevan J, Khrestian CM, Cakulev I, Markowitz A, Waldo AL. Simultaneous biatrial high-density (510-512 electrodes) epicardial mapping of persistent and long-standing persistent atrial fibrillation in patients: New insights into the mechanism of its maintenance. *Circulation*. 2015;132:2108-2117

Table 1:

Pt	Previous procedures	Previous Ablation Hx	LA Volume/cc^3	AT maps	Total Carousels
1	1	PVI + Roof + MI	111	1	0
2	3	PVI + CFAE + Roof	124	1	3
3	2	PVI + CFAE + MI	132	1	1
4	2	PVI	128	2	13
5	3	PVI + Roof + Anterior MI + anterior isthmus	120	1	2
6	4	PVI + CFAE + Floor + Septum + GPs	69	1	2
7	3	Surgical AF (Epicor) + LAA + RPV	156	1	0
8	2	PVI + CFAE	99	2	4
9	2	PVI + Anterior isthmus + Roof	162	1	2
10	1	PVI + MI	134	3	6
11	1	Roof line	178	3	6
12	1	Roof line + LLPV isolation	203	1	1
13	2	PVI + Roof + CFAE	148	1	0
14	1	PVI	117	3	9
15	2	PVI + MI + Roof	228	1	1

LA=left atrium; AT=Atrial Tachycardia

Table 2: A summary of the different carousel types and their distinguishing features

Category	Type I – Localized re-entry	Type II – pseudo-reentry	Type III – artifact
Macroscopic activation	Moves away in all directions	Incoming wavefront from elsewhere observed to head into the carousel, and advance activation around it	Interpolation in areas of low density.
Core (Scar threshold <0.03mV)	Area of grey ~1cm.	Pinwheel, or area of grey	Pinwheel
Cycle Length mapped	EGMS around carousel encompass full TCL	EGMs cannot be tracked around TCL owing to unaccounted isoelectric period between split potentials	Annotation encompasses TCL by chance
Electrograms	Fractionation within carousel usually critical site for ablation	Overlapping regions of split or fractionated potentials coinciding with wavefront collision.	Unipolar/bipolar EGMs suggestive of poor catheter contact, noise or movement artifact.
Map annotation display	Consistent pattern on bipolar and unipolar display	Consistent pattern on bipolar and unipolar display.	Inconsistent pattern on bipolar and unipolar annotation display.
Trouble-shooting		Careful interpretation of collision point and appreciation of split potentials	Can be removed by adjusting the confidence mask.

Figure legends

Figure 1 (and supplementary video 1): Putative sites of LR were identified as continuous rotational activation around an area <2cm (a pinwheel in this case), where each rotation encompassed one full tachycardia cycle length (TCL). This pattern of activation was labeled a "carousel". On the static LAT map, carousels were identified as sites that spanned the full spectrum of the color coded map (per the colors of the rainbow), running from red to purple, where the site of earliest activation (red) met the site of latest activation (purple).

Figure 2 (and supplementary video 2): A patient with previous pulmonary venous isolation and electrogram defragmentation for PsAF, as well as linear lesions for both peri-mitral and roof dependent ATs underwent redo atrial tachycardia (CL 280ms) ablation. The previous peri-mitral AT was treated with 2 lines (LLPV - posterior mitral annulus, RSPV - anterior mitral annulus), and the roof dependent AT with an anterior roof line. (a) The original roof line appeared incomplete as suggested by the ablation tags, (b) with the potential to set up LR. (c) 28,365 electro-anatomical points were collected in 41mins. (d) The activation map showed the full colour spectrum rotating counter-clockwise around a small island of scar (12mm, 55mm^2) on the anterior wall, akin to a carousel. (e) Electrograms sampled around this small circuit (1-6) contained very low voltage (0.05mV-0.15mV) and fractionated signals, and electrograms could be tracked around the circuit covering the full cycle length. Ablation delivered within the circuit terminated AT. Notably, some of the fractionation in EGM 3 is likely bystander, as it extends beyond local signal at EGM 4 and 5. (RUPV – right upper pulmonary vein; RLPV – right lower

pulmonary vein; LUPV – left upper pulmonary vein; LAA – left atrial appendage; MA – mitral annulus).

Figure 3 (and supplementary video 3): A further example of type I localized re-entrant AT (263ms) from a patient with previous pulmonary venous isolation, roof line and anterior mitral isthmus line. 26,978 electro-anatomical points were collected in 51mins. The activation map showed the full colour spectrum rotating counter-clockwise around an island of scar (9mm, 29mm^2) beneath the left sided veins. Electrograms sampled around this small circuit (1-6) covered the full cycle length. Fractionation within the circuit spanned 50% of the TCL. Ablation delivered within the circuit terminated AT. (RUPV – right upper pulmonary vein; RLPV – right lower pulmonary vein; LUPV – left upper pulmonary vein; LLPV – left lower pulmonary vein; LAA – left atrial appendage).

Figure 4 (and supplementary video 4): A patient with previous pulmonary venous isolation underwent mapping for a rapid AT (CL 150ms). 34,524 electro-anatomical points were collected in 56mins. A carousel was evident on the posterior mitral annulus with a pinwheel present at the center of rotation. This is captured in the static LAT map (top left) and magnified (top center). Upon closer inspection, the true nature of the carousel became apparent. This has been illustrated in the timing panels of propagation, which preserves the color coded display and demonstrates the leading edge of the activation wavefront in maroon. The dotted arrow represents where activation has been in the preceding timing panels. At time 0ms-65ms, a primary activation wavefront (labeled 1) travelling leftwards towards the mitral annulus turned clockwise through an area of slow conduction (sites 1-3) characterized by electrogram fractionation (right panel). A

secondary wavefront (labeled 2) travelled in from the roof and collided with the head of the primary wavefront (starred, characterized by a region of split potentials on one end - sites 6-7), and advanced activation around (site 9) creating the impression of complete rotation. Electrograms could not be tracked around the full TCL, owing to the unaccounted for isoelectric period between the split potentials. The presence of this incoming wavefront allows the operator to immediately discount this carousel as an active circuit. (RLPV – right lower pulmonary vein; LLPV – left lower pulmonary vein; LAA – left atrial appendage, MA – mitral annulus)

Figure 5 (and supplementary video 5): A further example of pseudo-reentry from a patient with multiple previous ablations and stable AT (CL 260ms). Carousel activation was seen on the anterior wall near an area of low voltage tissue, rotating around a pinwheel. This is captured in the static LAT map (top left) and magnified (top center). This was misdiagnosed as LR and extensively ablated without change in tachycardia activation (far right). An explanation for pseudo-reentry has been illustrated in the timing panels of propagation, which preserves the color coded display and demonstrates the leading edge of the activation wavefront in maroon. The dotted arrow represent where activation has been in the preceding timing panels. Between time 0ms-92ms, a primary wavefront of activation (labeled 1) travelling towards the mitral annulus encountered a line of block (sites 3-5), characterized by a regions of split potentials (EGM panel). The wavefront turned counter-clockwise around this line into a cul-de-sac (site 6). A secondary wavefront (labeled 2) travelling towards this area of low voltage collided with the head of the primary wavefront (starred – site 7), and advanced activation around (site 1-2) creating the impression of reentry. (RUPV – right upper pulmonary vein; LUPV – left upper pulmonary vein; LAA – left atrial appendage; MA – mitral annulus).

Figure 6 (and supplementary video 6): Carousel activation can be seen from just 3 closely spaced points with different annotation of local activation timing (LAT) across the window of interest (WOI) owing to interpolation between these three timings.

Figure 7 (and supplementary video 7): (a) A carousel was seen within an area of low voltage signal rotating around a pinwheel. (b) Bipolar electrograms 1-3 cover the tachycardia cycle length. However, site 3 signal was erroneous, as evident by the broad and blunt appearance in comparison to the other fractionated signals, and this was confirmed upon analysis of the unipolar signals (UNI1, UNI2) from which it was derived. It was incorporated into the activation map owing to interpolation in an area of incomplete mapping near the mitral annulus. (c) By removing the noise signal, carousel activation was no longer evident.

Figure 1: Carousel activation

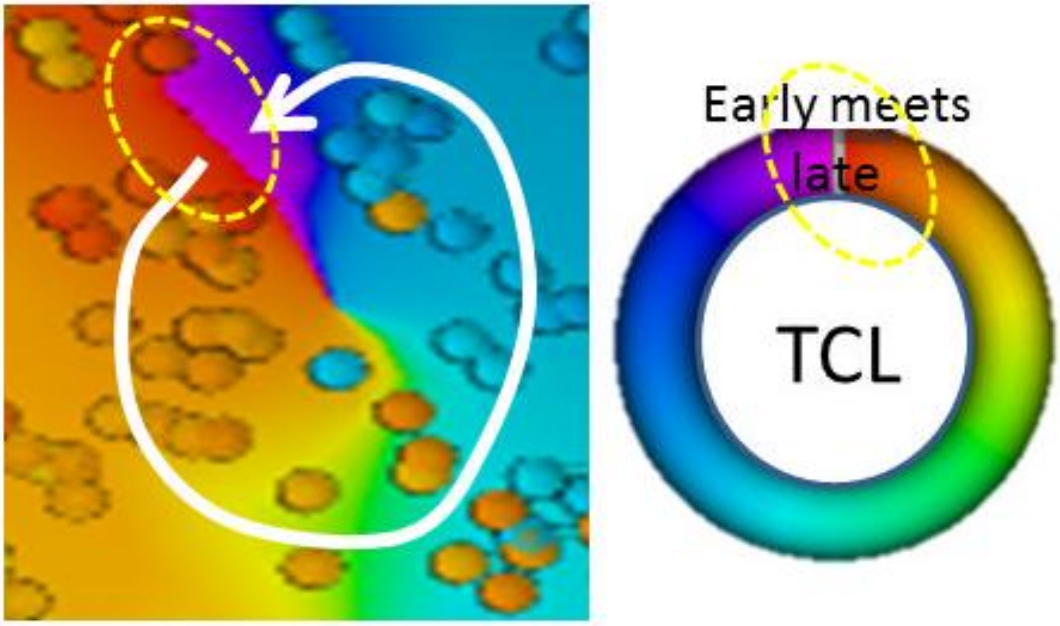

Figure 2: Type I Carousel - localized re-entry directly attributable to gaps in previous ablation line

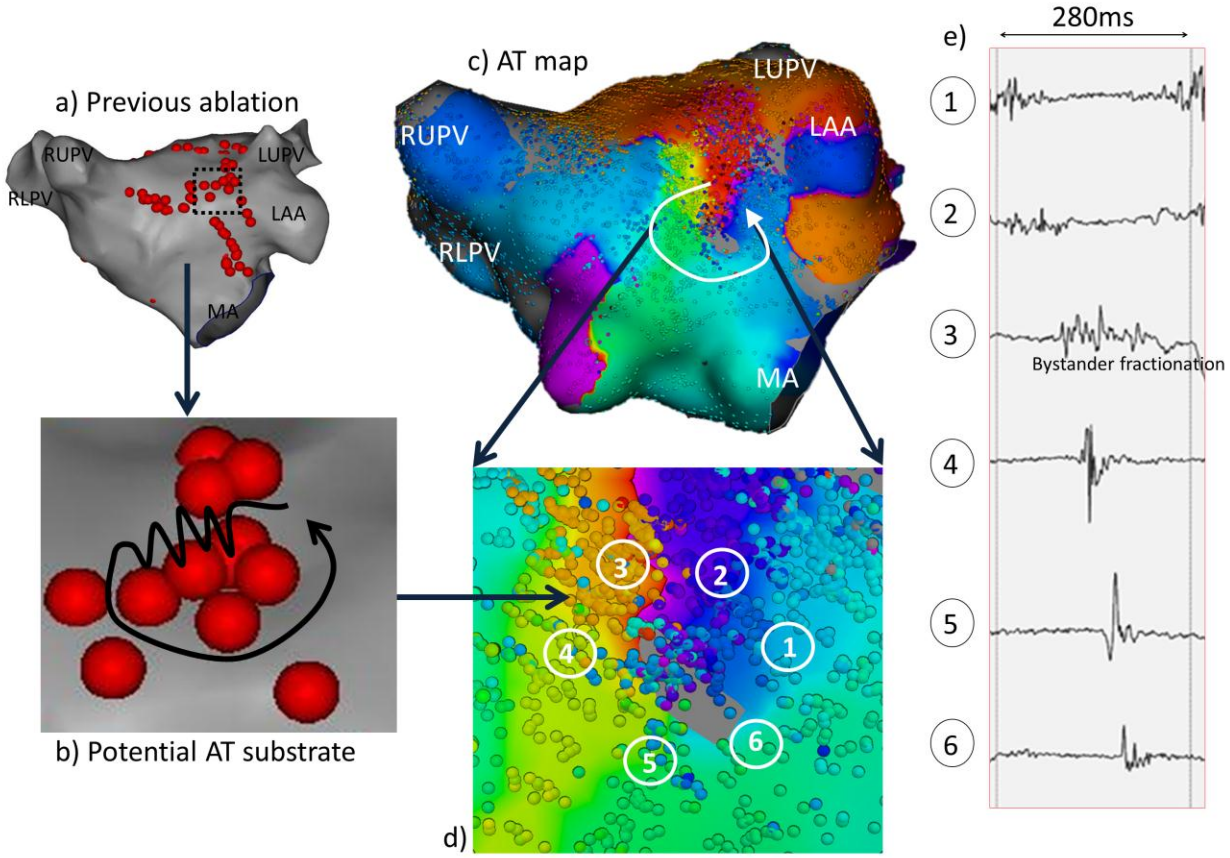

Figure 3: Type I carousel - localized re-entry inferior to the left pulmonary veins

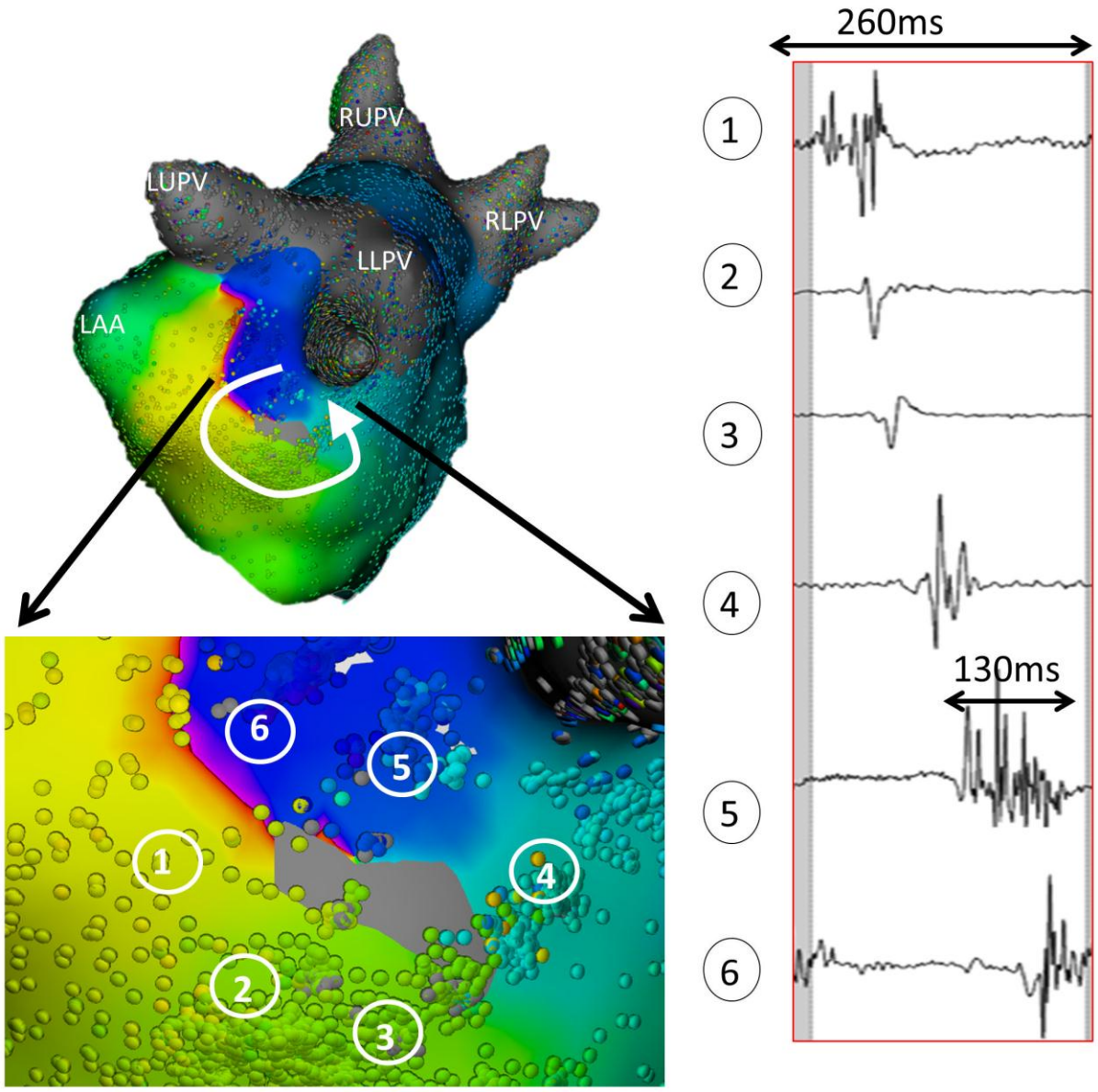

Figure 4: Type II Carousel – pseudo re-entry on the posterior mitral isthmus

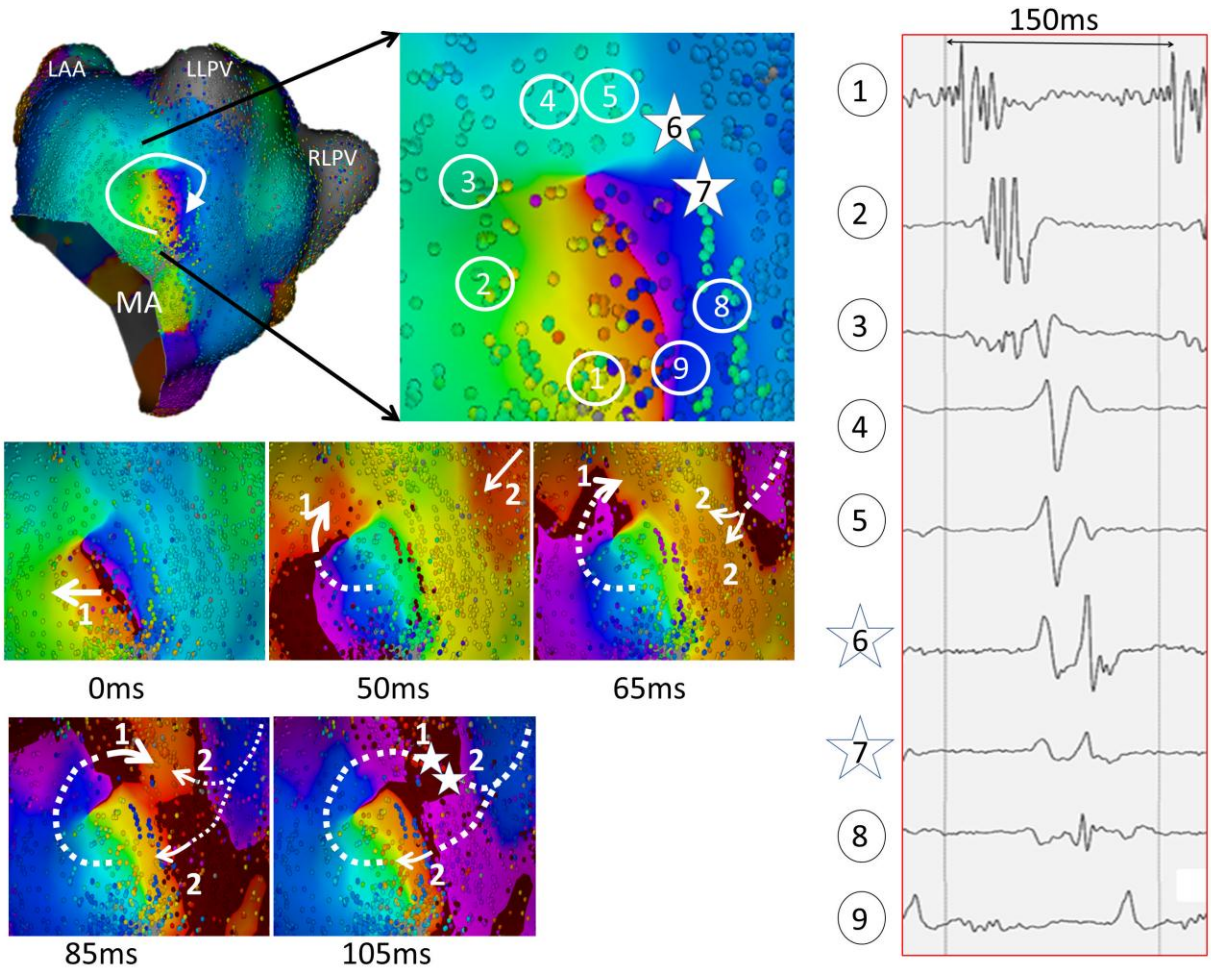

Figure 5: Type II Carousel – pseudo re-entry on the posterior mitral isthmus

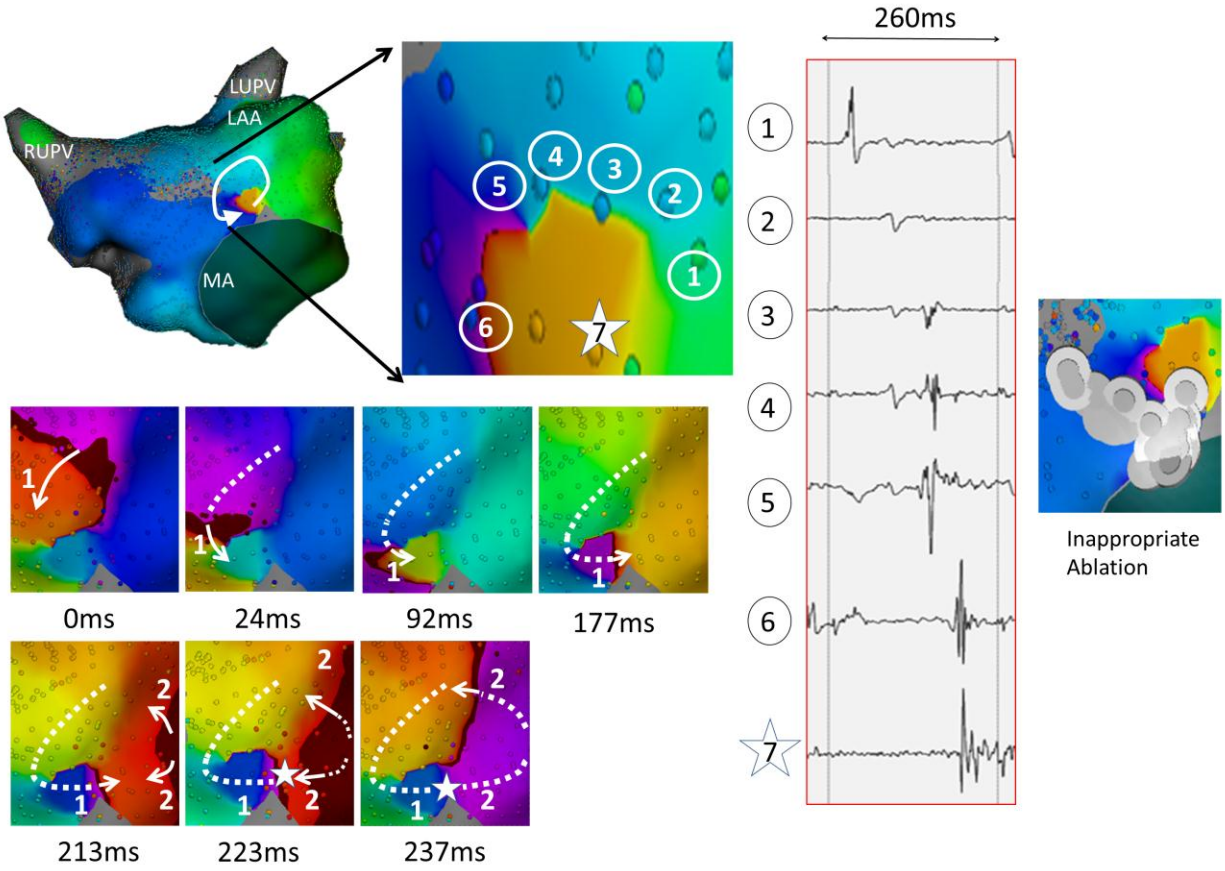

Figure 6: Type III Carousel – a function of interpolation

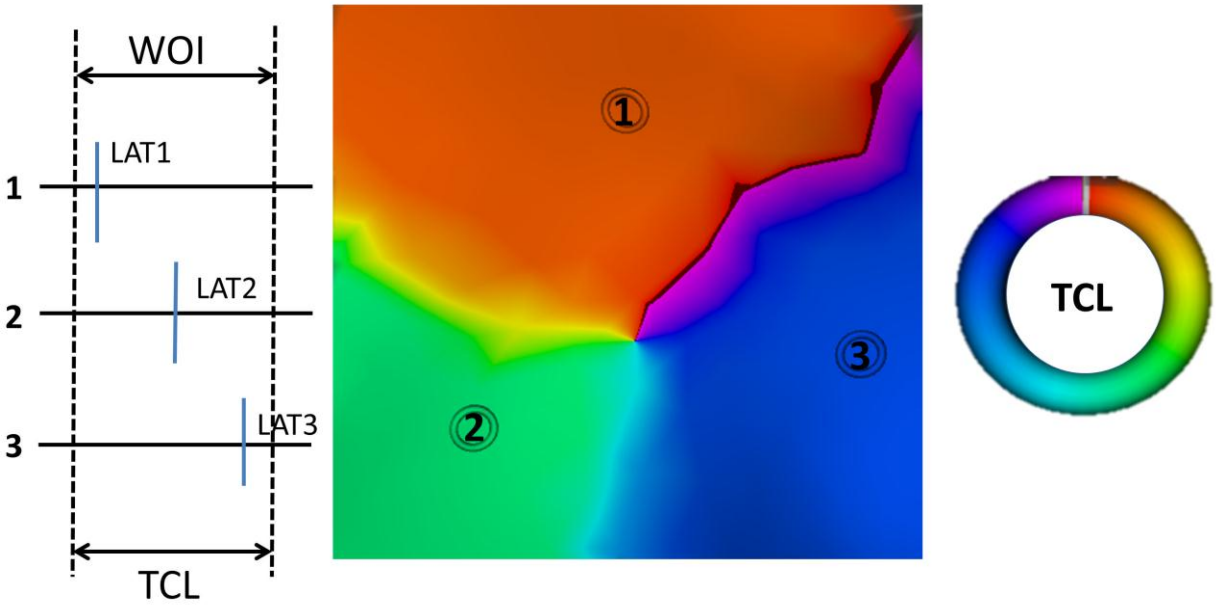

Figure 7: Type III Carousel - Artifact